

Article

Adaptive Neural Network Tracking Control of Robotic Manipulators Based on Disturbance Observer

Tianli Li ¹ , Gang Zhang ^{1,2,*}, Tan Zhang ² and Jing Pan ¹

¹ School of Electrical Engineering, Anhui Polytechnic University, Wuhu 241000, China; 2021030019@mail.wxc.edu.cn (T.L.); jingpan1102@126.com (J.P.)

² Anhui Undergrowth Crop Intelligent Equipment Engineering Research Center under Grant, Lu'an 237012, China; 42000028@wxc.edu.cn

* Correspondence: zhanggang@wxc.edu.cn; Tel.: +86-18156491056

Abstract: This article presents an adaptive neural network (ANN) control scheme based on a disturbance observer that can achieve trajectory tracking control of robotic manipulators under external disturbances and dynamic model uncertainties. Firstly, an ANN controller based on full-state feedback is derived using the backstepping technique to achieve an online approximation of uncertainty. The integral sliding mode surface with a position error is introduced into the controller, which reduces the steady-state error of the system and enhances robustness. Then, a novel disturbance observer is designed to estimate both the approximation errors of the ANN and external disturbances, and to provide compensation for the controller, effectively suppressing the trajectory tracking errors caused by approximation errors and disturbances. Subsequently, the Lyapunov stability theory is utilized to demonstrate the stability of the developed control strategy and the boundedness of all closed-loop signals. Finally, numerical simulations are used to confirm the efficacy of the proposed control method.

Keywords: adaptive neural network control; full-state feedback control; disturbance observer; robotic manipulator; backstepping sliding mode



Citation: Li, T.; Zhang, G.; Zhang, T.; Pan, J. Adaptive Neural Network Tracking Control of Robotic Manipulators Based on Disturbance Observer. *Processes* **2024**, *12*, 499. <https://doi.org/10.3390/pr12030499>

Academic Editor: Francisco Vazquez

Received: 22 January 2024

Revised: 20 February 2024

Accepted: 26 February 2024

Published: 28 February 2024



Copyright: © 2024 by the authors. Licensee MDPI, Basel, Switzerland. This article is an open access article distributed under the terms and conditions of the Creative Commons Attribution (CC BY) license (<https://creativecommons.org/licenses/by/4.0/>).

1. Introduction

With the improvement of robot technology and automation levels, the research on robot control systems has attracted widespread attention [1–5]. The robotic manipulator can be regarded as a multivariable, strongly coupled, and uncertain nonlinear system, which is susceptible to model parameter perturbations and unknown nonlinearities. In recent years, adaptive neural networks (ANNs) have received increasing attention and have been designed as approximation controllers for nonlinear uncertain systems. Furthermore, ANN control methods have been successfully applied to the full-state feedback control and output feedback control of nonlinear systems [6], the asymptotic stability of tracking errors for aircraft and autonomous underwater vehicles [7,8], and robot motion control [9], etc.

Many control schemes have been successfully applied to robotic systems with complex control problems. Based on the calculation torque control method, a linear model of the robotic system was obtained, and a fractional order PID controller was designed to improve the anti-interference ability of the tracking system [10]. However, PID controllers do not meet the high-precision control requirements of robot systems with nonlinear and time-varying characteristics. In [11,12], a robust control method was introduced into the nonlinear mechanical system of constrained robots, but [12] can only guarantee that the time-varying bounded constraints were satisfied. To achieve accuracy in tracking the position of human hands, an adaptive impedance control was proposed by combining nonlinear control theory with dynamic models to guarantee the safety of human-robot interaction [13]. In [14], it uses saturation functions instead of sign functions and quasi-sliding modes, and compared with the sign function with ideal switching characteristics,

the input torque curve based on the saturation function is smoother and can weaken the system's chattering. A new sliding mode controller has been developed considering the kinematic and dynamic models of nonlinear robots, which can meet the requirements of motion speed and direction [15]. Although the above methods can meet the control requirements, the uncertainty of the model and the external unknown disturbances remain challenging issues.

In recent years, sliding mode control (SMC) has been widely used due to its strong robustness to external disturbances and model uncertainties [14,16]. Furthermore, in order to improve the adaptive control design of systems, neural network (NN) control and fuzzy control have been studied due to their strong approximation ability. The adaptive fuzzy SMC was studied for robots [17–19]. A fuzzy control design lacks systematicity and may reduce the control accuracy of the system, while ANN control has a simple structure and can approximate nonlinear functions with arbitrary precision. In [20], a comprehensive description was given of a composite control strategy combining SMC and NNs, which can be used to improve the tracking control of nonlinear robot systems. In [21,22], an ANN scheme for the trajectory tracking control of robotic manipulators was designed, and the barrier Lyapunov function was introduced to handle output error constraints/full state constraints. Moreover, [21] used a RBFNN to approximate the lumped uncertainty including external disturbances, and add an auxiliary system to the controller to reduce the impact of input saturation. In [22], the effects of actuator saturation and time-varying delay were eliminated. A neural network-based backstepping SMC method was studied, which utilized backstepping SMC to compensate for input saturation and applied NN control to approximate model uncertainty online [23]. Ref. [24] presented a neural network-based SMC for n-link robots with an input dead zone and delay constraints. Furthermore, error translation functions were added to the sliding surface to improve tracking accuracy, and obstacle functions were used to solve state constraint problems. Ref. [25] designed an ANN controller combined with symmetric barrier Lyapunov function, which utilizes the continuous updating of network weights to approximate unknown nonlinear dynamics. In addition, SMC was added to the backstepping design to eliminate the chattering phenomenon of the system. From the above analysis, the method of combining ANNs with SMC makes the system have strong anti-interference ability and robustness.

Disturbance observers are widely used to handle uncertain disturbances in nonlinear systems, typically combined with control methods. Uncertain nonlinear systems with linear parameters can be solved by combining the NN control techniques that have been presented recently with conventional adaptive control and backstepping control. Based on the above research, it is necessary to combine disturbance observer technology with NN control to solve the tracking control problem of nonlinear robot systems. A composite controller combining the observer control method with a sliding mode control and a neural network was designed to achieve control objectives for nonlinear systems [26–29]. In [26], it introduces the use of optimization methods to obtain the optimal weights of the NN observer, which reduces the workload of adjusting parameters. Then, the position and speed of the robot were estimated using observers. This scheme makes the changes in control inputs smoother. In [27,29], disturbance observers were utilized to handle unknown models and disturbances, but [27] was not applicable in the presence of measurement noise. To achieve the feedback control of gyroscope output, Ref. [30] developed ANNs and disturbance observers to address the problems of nonlinear dynamics, environmental fluctuations, and external disturbances. To enhance robustness, the SMC method was introduced. An observer-based ANN impedance control method was studied for constrained robotic manipulators [31], where the disturbance observer was used to eliminate unknown disturbances and the ANN was employed to solve unknown dynamic models. Under the action of the controller, the robot exhibits a given ideal impedance relationship in its interaction with the outside world. In the above discussion, most control methods require a large amount of online computation, and disturbance observers are only utilized to handle external disturbances without fully considering the approximation errors of ANNs. Based

on this, an ANN control strategy based on disturbance observer compensation is studied in this paper. This article first uses an ANN controller to approximate model uncertainty. We further design a new disturbance observer to simultaneously estimate approximation errors and external disturbances, which is different from previous work. Subsequently, we update this estimated value into the designed controller to provide compensation.

By combining the recently proposed neural network control methods with adaptive control and backstepping techniques, uncertain nonlinear systems with linear parameters can be solved. The main contributions of the algorithm proposed in this article are as follows:

- (1) A novel adaptive neural network controller combining a disturbance observer is designed to simultaneously solve the uncertain parts of the model and environmental disturbances. Compared to [6], an ANN controller is derived using backstepping technology, and a sliding mode surface with an integral term is added to the virtual control law. This reduces the steady-state errors of the system and enhances its robustness without increasing its energy consumption.
- (2) The bounded value of approximation error is introduced in the observer structure, which can accurately estimate the approximation error of the ANN and ensure the stability of the observer. When designing the observer, considering the online approximation of uncertainty by the adaptive update law, the state equation of the system is rewritten.
- (3) Unlike [27,29,31], in addition to estimating external disturbances, the designed disturbance observer can also handle the approximation errors of NNs. The uniform boundedness of all signals in the closed-loop system is proved using the Lyapunov stability theorem.

The rest of this article is constructed as follows: Section 2 introduces the description of the problem and preparation. Section 3 provides a detailed process and stability analysis of the control law design. The numerical simulation of a robotic manipulator with two degrees is presented in Section 4. Finally, the conclusions of the research are drawn in Section 5.

2. Preliminaries and Problem Description

2.1. Preliminaries

Notation 1. $(\cdot)^T$ denotes the transpose matrix, $|\cdot|$ represents the absolute value, and $\|\cdot\|$ means the Euclidean norm.

Lemma 1 ([32]). *If there exists a continuous positive differentiable function $V(x)$ that satisfies $\kappa_1(\|x\|) < V(x) < \kappa_2(\|x\|)$ (κ_1 and κ_2 belong to class K functions) and has a bounded initial condition, if $\dot{V}(x) \leq -\rho V(x) + C$, where $\rho, C > 0$, then $V(x)$ is bounded and the solution $x(t)$ is uniformly bounded.*

Lemma 2 ([32]). *Let $Q \in R^{n \times n}$ be a positive semi-definite symmetric matrix; therefore, all the eigenvalues of Q are positive real numbers. There exists $\lambda_{\min}\|x\|^2 \leq x^T Q x \leq \lambda_{\max}\|x\|^2$, $\forall x \in R^n$, where λ_{\min} and λ_{\max} are the minimum and maximum eigenvalues of Q .*

Definition 1 ([33]). *Semi-globally uniformly bounded (SGUB): Consider a generalized nonlinear system $\dot{\psi} = f(\psi, t)$, $\psi \in R^n$, $t \geq t_0$. For any compact set Ω_i and initial state $\psi(t_0) \in \Omega_i$, if there is a constant $\mu > 0$ and a time constant $T(\xi, \psi(t_0))$, it satisfies $\|\psi(t)\| \leq \mu$, $\forall t \geq t_0 + T(\xi, \psi(t_0))$. We define the system state $\psi(t)$ as SGUB.*

2.2. Neural Networks

Any continuous function $f_i(Z)$ can be approximated by a neural network, which can be represented as

$$\begin{aligned} f_i(Z) &: R^q \rightarrow R, \\ f_i(Z) &= W_i^T S_i(Z), i = 1, 2, \dots, n \end{aligned} \quad (1)$$

where $Z = [Z_1, \dots, Z_q]^T$ is the input of NNs, $W_i = [\omega_1, \dots, \omega_n]^T$ is the weight vector, and $N > 1$ denotes the number of nodes in the NN, $S_i(Z) = [S_1(Z), \dots, S_N(Z)]^T$ represents the basis function vector.

According to the definition [6], we know that there exists an optimal weight $W_i^* = [W_i^*, \dots, W_n^*] \in R^{N \times n}$, and given the function $f_i(Z)$ on the compact set $Z \in \Omega \subset R^q$, it can be approximated with arbitrary accuracy through the output of the NNs.

$$f_i(Z) = W_i^{*T} S_i(Z) + \varepsilon_i(Z), i = 1, 2, \dots, n \quad (2)$$

where $\varepsilon_i(Z) = [\varepsilon_1(Z), \dots, \varepsilon_n(Z)]^T$ is the approximation error, which is bounded and satisfies $|\varepsilon_i(Z)| \leq \bar{\varepsilon}_i, \forall Z \in \Omega$, where $\bar{\varepsilon}_i$ is an unknown positive constant. And W_i^* satisfies

$$W_i^* := \arg \min_{W_i \in R^N} \left\{ \sup_{Z \in \Omega} |f_i(Z) - W_i^T S_i(Z)| \right\}.$$

The selected Gaussian function is represented as

$$S_i(Z) = \exp\left(-\frac{\|z - \mu_i\|^2}{\eta_i^2}\right), i = 1, \dots, N \quad (3)$$

where μ_i and η_i are the center position and width of the i -th neuron, respectively.

Remark 1. According to the expression of W_i^* , which is defined as the value W_i that minimizes $|\varepsilon_i(Z)|$, the selection of parameters in Gaussian functions will have an impact on $\varepsilon_i(Z)$. Considering the optimal weight W_i^* , we can obtain $|f_i(Z) - \hat{f}_i(Z, W^*)| = |\varepsilon_i(Z)| \leq \bar{\varepsilon}_i$.

2.3. Problem Description

The dynamics of an n -link rigid robotic manipulator are as follows [6].

$$M(q)\ddot{q} + C(q, \dot{q})\dot{q} + G(q) = \tau(t) - J^T(q)f(t) \quad (4)$$

where $q \in R^n$ represents the position vector, $M(q) \in R^{n \times n}$ is the inertia matrix of the robotic manipulator, which is positively definite and symmetric, $C(q, \dot{q})\dot{q} \in R^{n \times n}$, $G(q) \in R^n$ denotes the Coriolis-centripetal torque and the gravity vector, respectively. $\tau(t) \in R^n$ denotes the control input torque of the system. $J(q)f(t)$ is the product of the Jacobian matrix and the external forces exerted by humans and the environment.

Property 1 ([6]). $\dot{M}(q) - 2C(q, \dot{q})$ is a skew-symmetric matrix.

Assumption 1. The nonlinear term $f(t)$ is supposed to be constrained, bounded and slowly varying, it satisfies $\|f(t)\| \leq \bar{f}$, where \bar{f} is a positive constant.

Let $x_1 = q = [x_{11}, \dots, x_{1n}]^T$ and $x_2 = \dot{q} = [x_{21}, \dots, x_{2n}]^T$, and the integrated system can be rewritten as

$$\begin{cases} \dot{x}_1 = x_2 \\ \dot{x}_2 = M^{-1}(x_1)(\tau - J^T(x_1)f(t) - C(x_1, x_2)x_2 - G(x_1)) \end{cases} \quad (5)$$

The control objective is to design a controller that enables the system variable q to accurately track the set desired trajectory $x_d(t) = [q_{d1}(t), \dots, q_{dn}(t)]^T$ while ensuring that

the error of constraint converges to the zero domain. The desired trajectory $x_d(t)$ is bounded and differentiable. In the following, we abbreviate $M(x_1)$ as M , $C(x_1, x_2)$ as C , and $G(x_1)$ as G .

Remark 2. In actual operation, robotic manipulators are easily affected by parameter perturbations and external disturbances, so it is necessary to consider the uncertainty of $C(q, \dot{q})\dot{q}$ and $G(q)$ in their models. The forces that interact between the robot and its surroundings are mostly responsible for the external disturbances of the model. Due to the extremely short duration of the interaction force, it does not affect the system's overall convergence; rather, it solely influences the estimated value or tracking error of the disturbance during the operating time. The force $f(t)$ is bounded because of the constraints imposed by the robot's physical structure. The above Assumption 1 is reasonable. We reasonably assume that the model errors, desired trajectories, and disturbances are limited because the joint angles and velocities of the robotic manipulator are bounded.

3. Main Results

3.1. Controller Design

In this section, an ANN full-state feedback control strategy for nonlinear robotic systems is proposed to handle uncertainty. Subsequently, under the action of the newly designed observer, disturbances and approximation errors are resolved, which is different from existing research. The block diagram of the tracking control scheme is depicted in Figure 1.

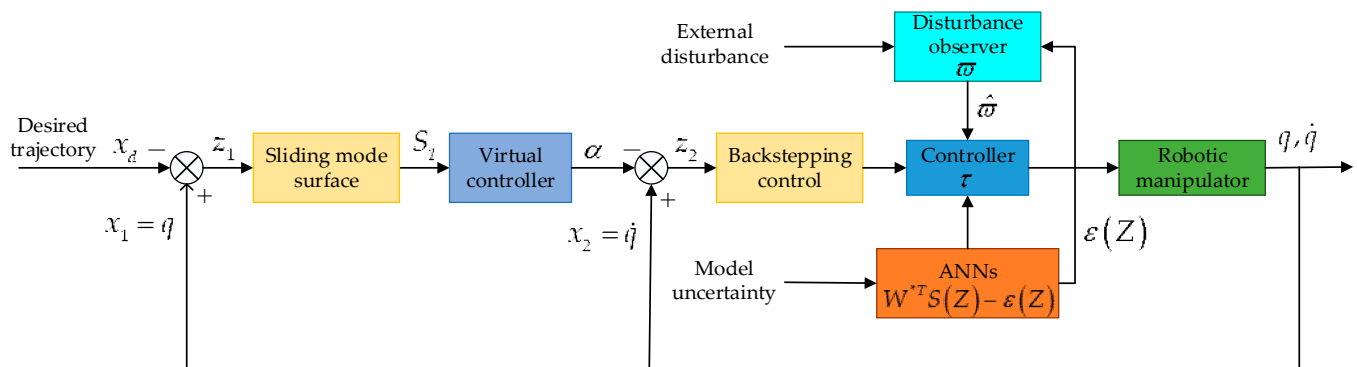


Figure 1. Block diagram of ANN control.

To begin with, we define the generalized tracking errors $z_1(t)$ and $z_2(t)$ as

$$\begin{aligned} z_1(t) &= [z_{11}(t), \dots, z_{1n}(t)]^T = x_1(t) - x_d(t) \\ &= [x_{11}(t) - q_{d1}(t), \dots, x_{1n}(t) - q_{dn}(t)]^T \end{aligned} \quad (6)$$

$$\begin{aligned} z_2(t) &= [z_{21}(t), \dots, z_{2n}(t)]^T = x_2(t) - \alpha(t) \\ &= [x_{21}(t) - \alpha_1(t), \dots, x_{2n}(t) - \alpha_n(t)]^T \end{aligned} \quad (7)$$

where $\alpha(t) = [\alpha_1(t), \alpha_2(t), \dots, \alpha_n(t)]^T$ is the virtual controller to be introduced, which will be provided below.

The linear sliding surface can be designed as

$$S_1(t) = z_1(t) + K_1 \int_0^t z_1(t) dt \quad (8)$$

Design the virtual controller α as

$$\alpha = -K_1 z_1 - K_s S_1 + \dot{x}_d \quad (9)$$

where K_1 and K_s are positive-definite diagonal matrices, and we have

$$\dot{z}_1 = z_2 + \alpha - \dot{x}_d = z_2 - K_1 z_1 - K_s S_1 \quad (10)$$

According to (5) and (9), the derivative of z_2 is

$$\dot{z}_2 = M^{-1} \left(\tau - J^T f(t) - Cx_2 - G \right) - \dot{\alpha} \quad (11)$$

Then, the time derivative of $S_1(t)$ is

$$\dot{S}_1 = \dot{z}_1 + K_1 z_1 = z_2 + \alpha - \dot{x}_d + K_1 z_1 \quad (12)$$

A model-based controller τ_0 is designed as

$$\tau_0 = -S_1 - K_2 z_2 + J^T f(t) + C\alpha + G + M\dot{\alpha} \quad (13)$$

where K_2 is the positive-definite diagonal matrix.

The Lyapunov function candidate V_1 is chosen as

$$V_1 = \frac{1}{2} S_1^T S_1 + \frac{1}{2} z_2^T M z_2 \quad (14)$$

Differentiating V_1 yields

$$\begin{aligned} \dot{V}_1 &= -S_1^T K_s S_1 + S_1^T z_2 + \frac{1}{2} z_2^T (\dot{M} - 2C) z_2 + z_2^T (\tau_0 - J^T f(t) - C\alpha - G - M\dot{\alpha}) \\ &= -S_1^T K_s S_1 + S_1^T z_2 + z_2^T (\tau_0 - J^T f(t) - C\alpha - G - M\dot{\alpha}) \end{aligned} \quad (15)$$

Remark 3. According to Property 1 and the definition of skew-symmetric matrices, we have $\frac{1}{2} z_2^T (\dot{M} - 2C) z_2 = 0$. By substituting (13) into (15), we have $\dot{V}_1 = -S_1^T K_s S_1 - z_2^T K_2 z_2$, and the sliding mode surface $S_1(t)$ will converge to zero, that is, $S_1(t) = 0$. Subsequently, according to (12), we have $\dot{S}_1 = \dot{z}_1 + K_1 z_1 = 0$, and the tracking error z_1 will converge to zero.

A robotic manipulator is a nonlinear and complex system. In actual control processes, it is difficult to obtain accurate dynamic models, and uncertainty exists in $C(x_1, x_2)$, $G(x_1)$, and $f(t)$. In the actual operation process, the model-based controller τ_0 designed in (13) may not be able to achieve the control objectives. Therefore, ANNs are introduced to compensate for unknown dynamic model parameters and improve tracking accuracy. The ANN controller τ is designed as

$$\tau = -S_1 - K_2 z_2 + J^T f(t) + \hat{W}^T S(Z) + M(x_1) \dot{\alpha}(t) \quad (16)$$

where $S(Z)$ is the radial basis function, and $Z = [x_1^T, x_2^T, \alpha^T, \dot{\alpha}^T]$ are the input variables of the NN. \hat{W} and W^* are the estimated and optimal weights of the NN, and the error between them is defined as $\tilde{W} = \hat{W} - W^*$. The optimal weight is constructed for the convenience of derivation and analysis, and $\hat{W}^T S(Z)$ is utilized to estimate $W^{*T} S(Z)$,

$$C(x_1, x_2) \alpha(t) + G(x_1) = W^{*T} S(Z) - \varepsilon(Z) \quad (17)$$

where $\varepsilon(Z) \in R^n$ is the approximation error.

The weight adaptive law \hat{W}_i of NNs is designed as

$$\dot{\hat{W}}_i = -\Gamma_i (S(Z) z_{2,i} + \sigma_i \hat{W}_i) \quad (18)$$

where σ_i is a small positive constant used to improve robustness, and Γ_i is a positive definite gain matrix.

Remark 4. Due to the boundedness of x_1 , x_2 , x_d , and \dot{x}_d , it can be concluded that the sliding mode surface $S_1(t)$ and virtual control α given in (8) and (9) are bounded. Considering that the NN $\hat{W}^T S(Z)$ is bounded, the adaptive controller τ in (16) is also bounded. It is worth mentioning that if the value of one of $C(x_1, x_2)$ and $G(x_1)$ is precisely known, we can exclude this term from (17) and rewrite this part in (16).

To handle the approximation error and time-varying disturbance of the ANN in (16), a new disturbance observer is proposed to accurately estimate $\varepsilon(Z)$ and $J^T f(t)$. Firstly, based on the research in the previous chapter, the state Equation (5) can be rewritten as

$$\begin{cases} \dot{x}_1 = x_2 \\ \dot{x}_2 = M^{-1}(x_1)(\tau - \hat{W}^T S(Z)) + M^{-1}(x_1)\omega \end{cases} \quad (19)$$

where $\omega = -J^T f(t) - \varepsilon(Z)$ represents the external disturbances of the system and the approximation errors of ANNs.

Remark 5. While ensuring the convergence of z_2 , according to (7), (16), and (17), we have $C(x_1, x_2)x_2 + G(x_1) \approx C(x_1, x_2)\alpha(t) + G(x_1) = \hat{W}^T S(Z) + \varepsilon(Z)$. x_2 exists in model uncertainty, and the ANN control processes it first to make the tracking error $z_2 = x_2 - \alpha$ converge to the small neighborhood of zero. Therefore, when designing the observer, we can reasonably approximate x_2 as .

Then, the disturbance observer is designed as

$$\dot{\hat{\omega}} = l(x) \left(M(x_1)\dot{x}_2 + \hat{W}^T S(Z) + \bar{\varepsilon} - \tau - \hat{\omega} \right) \quad (20)$$

where $l(x) = \text{diag}\{l_{11}, l_{12}, \dots, l_{1n}\} > 0$ is a nonlinear gain matrix, to simplify the derivation, $l(x)$ is designed as a linear function vector. $\hat{\omega}$ is the estimated observation value of ω . The designed disturbance observer (20) may not complete the control goal, and this is because it requires angular acceleration signals of the state, and system instability may result from obtaining acceleration signals by differentiating velocity signals. Therefore, this article has designed the following three steps to solve the above problems.

Step 1. Construct auxiliary functions and define the internal state variables of the observer as

$$\gamma = \omega - h(x) \quad (21)$$

where $\gamma \in R^n$ is the internal state variable of the observer, and $h(x) \in R^n$ represents the function vector to be designed. To avoid introducing acceleration signals, the gain matrix $l(x)$ and the $h(x)$ of the disturbance observer have the following relationship:

$$l(x)M(x_1)\dot{x}_2 = \frac{dh(x)}{dx} \quad (22)$$

Step 2. Design disturbance observer structure. According to (20)–(22), we have

$$\dot{\hat{\gamma}} = l(x) \left(\hat{W}^T S(Z) + \bar{\varepsilon} - \tau - \hat{\gamma} - h(x) \right) \quad (23)$$

We can obtain a disturbance observer without acceleration as

$$\begin{cases} \dot{\hat{\omega}} = \hat{\gamma} + h(x) \\ \dot{\hat{\gamma}} = l(x) \left(\hat{W}^T S(Z) + \bar{\varepsilon} - \tau - \hat{\gamma} - h(x) \right) \end{cases} \quad (24)$$

Remark 6. In the design process of the disturbance observer, in order to ensure the stability of the observer structure, an approximation error bounded value $\bar{\varepsilon}$ is added. Based on prior knowledge, we know that $|\varepsilon(Z)| \leq \bar{\varepsilon}$, $\forall Z \in \Omega$. The disturbance observer designed in [29] is $\dot{\hat{\omega}} = l(x)(M(x_1)\dot{x}_2 + C(x_1, x_2)x_2 + G(x_1) - \tau - \hat{\omega}')$, which only estimates and compensates for external friction without considering the approximation error $\varepsilon(Z)$. Unlike in [29], the observer designed in this article can simultaneously process $\varepsilon(Z)$ and $f(t)$.

Step 3. We define the observation error of the disturbance observer as

$$\tilde{\omega} = \omega - \hat{\omega} \quad (25)$$

According to (22)–(25), the derivative of $\tilde{\omega}$ is

$$\begin{aligned} \dot{\tilde{\omega}} &= \dot{\omega} - \dot{\hat{\omega}} \\ &= \dot{\omega} - \dot{\gamma} - \frac{dh(x)}{dx} \\ &= l(x)\hat{\omega} - l(x)(\hat{W}^T S(Z) + \bar{\varepsilon} - \tau) - l(x)M\dot{x}_2 \\ &= l(x)\hat{\omega} - l(x)(\hat{W}^T S(Z) + \bar{\varepsilon} - \tau) - l(x)(\tau - \hat{W}^T S(Z) + \omega) \\ &= -l(x)\tilde{\omega} - l(x)\bar{\varepsilon} \end{aligned} \quad (26)$$

It is difficult to obtain prior knowledge of disturbance differentiation in practical situations. We assume that the characteristic change of ω with respect to the disturbance observer is slow, there is $\dot{\omega} = 0$.

The design of an ANN controller τ based on the disturbance observer is as follows

$$\tau = -S_1 - K_2 z_2 + \hat{W}^T S(Z) + M(x_1)\dot{x}(t) - \hat{\omega} \quad (27)$$

Theorem 1. For the robot system described in (4), under the action of the adaptive neural network controller (27), all state variables can be measured and globally stable. For the initial compact set Ω_0 , where $(x_1(0), x_2(0), \hat{\omega}(0), \hat{W}_i(0), S_1(0)) \in \Omega_0$, the error signals z_1 , z_2 , $\tilde{\omega}$, and \tilde{W} and the sliding mode vector S_1 will always be in the compact sets Ω_{z_1} , Ω_{z_2} , $\Omega_{\tilde{\omega}}$, $\Omega_{\tilde{W}}$, and Ω_{S_1} :

$$\begin{aligned} \Omega_{z_1} &= \left\{ \|z_1\| \leq \sqrt{D} \right\} \\ \Omega_{z_2} &= \left\{ \|z_2\| \leq \sqrt{\frac{D}{\lambda_{\min}(M)}} \right\} \\ \Omega_{\tilde{\omega}} &= \left\{ \|\tilde{\omega}\| \leq \sqrt{D} \right\} \\ \Omega_{\tilde{W}} &= \left\{ \|\tilde{W}\| \leq \sqrt{\frac{D}{\lambda_{\min}(\Gamma^{-1})}} \right\} \\ \Omega_{S_1} &= \left\{ \|S_1\| \leq \sqrt{D} \right\} \end{aligned} \quad (28)$$

where $D = 2(V_2(0) + C/\rho)$, ρ and C are constants and satisfy $\rho > 0$ and $C > 0$.

Proof. A Lyapunov function V_2 is constructed as follows:

$$V_2 = \frac{1}{2} S_1^T S_1 + \frac{1}{2} z_2^T M z_2 + \frac{1}{2} \sum_{i=1}^n \tilde{W}_i^T \Gamma_i^{-1} \tilde{W}_i + \frac{1}{2} \tilde{\omega}^T \tilde{\omega} \quad (29)$$

By substituting (18), (19), (26), and (27) into the derivative of V_2 , we can obtain

$$\begin{aligned}
 \dot{V}_2 &= -S_1^T K_s S_1 + S_1^T z_2 + z_2^T [\tau - \hat{W}^T S(Z) + \omega - M\dot{\alpha}] \\
 &\quad + \sum_{i=1}^n \tilde{W}_i^T \Gamma_i^{-1} \dot{\tilde{W}}_i + \tilde{\omega}^T \dot{\tilde{\omega}} \\
 &\leq -S_1^T K_s S_1 + S_1^T z_2 + z_2^T [-S_1 - K_2 z_2 + \omega - \tilde{\omega}] \\
 &\quad + \sum_{i=1}^n \tilde{W}_i^T \Gamma_i^{-1} \dot{\tilde{W}}_i + \tilde{\omega}^T \dot{\tilde{\omega}} \\
 &\leq -S_1^T K_s S_1 - z_2^T K_2 z_2 - z_2^T \tilde{\omega} \\
 &\quad - \sum_{i=1}^n \tilde{W}_i^T \sigma_i \dot{\tilde{W}}_i + \tilde{\omega}^T (-l(x)\tilde{\omega} - l(x)\tilde{\varepsilon}) \\
 &\leq -S_1^T K_s S_1 - z_2^T \left(K_2 - \frac{1}{2}I\right) z_2 - \sum_{i=1}^n \frac{\sigma_i}{2} \|\tilde{W}_i\|^2 \\
 &\quad + \sum_{i=1}^n \frac{\sigma_i}{2} \|W_i^*\|^2 - \tilde{\omega}^T \left(\frac{1}{2}l(x) - \frac{1}{2}I\right) \tilde{\omega} + \frac{1}{2}l(x)\|\tilde{\varepsilon}\|^2 \\
 &\leq -\rho V_2 + C
 \end{aligned} \tag{30}$$

where

$$\rho = \min \left(2\lambda_{\min}(K_s), \frac{2\lambda_{\min}\left(K_2 - \frac{1}{2}I\right)}{\lambda_{\max}(M)}, \min \left(\frac{\sigma_i}{\lambda_{\max}(\Gamma_i^{-1})} \right), \lambda_{\min}(l(x) - I) \right) \tag{31}$$

$$C = \sum_{i=1}^n \frac{\sigma_i}{2} \|W_i^*\|^2 + \frac{1}{2}l(x)\|\tilde{\varepsilon}\|^2 \tag{32}$$

Through the above analysis, we can prove that signals z_1 , z_2 , $\tilde{\omega}$, \tilde{W} , and S_1 are semi-globally uniformly bounded.

By multiplying the left and right ends of the Equation (30) by $e^{\rho t}$ and integrating them on $[0, t]$, we can obtain

$$\begin{aligned}
 \dot{V}_2 e^{\rho t} &\leq -\rho V_2 e^{\rho t} + C e^{\rho t} \\
 \frac{d}{dt} (V_2 e^{\rho t}) &\leq C e^{\rho t} \\
 V_2 e^{\rho t} &\leq \frac{C}{\rho} e^{\rho t} + \left(V_2(0) - \frac{C}{\rho} \right) \\
 V_2 &\leq \left(V_2(0) - \frac{C}{\rho} \right) e^{-\rho t} + \frac{C}{\rho} \leq V_2(0) + \frac{C}{\rho}
 \end{aligned} \tag{33}$$

Then, we have

$$\frac{1}{2} \|z_1\|^2 \leq V_2(0) + \frac{C}{\rho} \tag{34}$$

From the above analysis, it can be found that z_1 converges to the compact set Ω_{z_1} , and similarly, it can be proven that z_2 , $\tilde{\omega}$, \tilde{W} , and S_1 converge to the compact sets Ω_{z_2} , $\Omega_{\tilde{\omega}}$, $\Omega_{\tilde{W}}$, and Ω_{S_1} , respectively.

The proof is completed. \square

3.2. Design Procedure

The design procedure of this scheme is summarized as follows:

1. Rewrite the system into the form of (5) using (4).
2. Set $x_d = [0.14 \sin(0.5t); 0.14 \cos(0.5t)]$ in (6) and choose $K_1, K_2, K_S > 0$.
3. Determine $S_1(t)$ and α from (8) and (9), and design τ_0 as the structure in (13), so that (15) satisfies $\dot{V}_1 < 0$.
4. Reconstruct $C(x_1, x_2)\alpha(t)$ and $G(x_1)$ in (13) to obtain the form of (16), and select appropriate values for Γ_i and σ_i in (18).
5. Build the system in the form of (19) using (5) and (17).
6. Choose $l(x) > 0$, and rebuild \hat{w} form (24).

7. Feedback the value of $\hat{\omega}$ in (24) to (16) to obtain the structure of (27).

4. Simulations

In this section, to illustrate the efficacy of the proposed control, simulation experiments were carried out on a robotic manipulator with two rotating joints in the vertical plane, as Figure 2 displays [22].

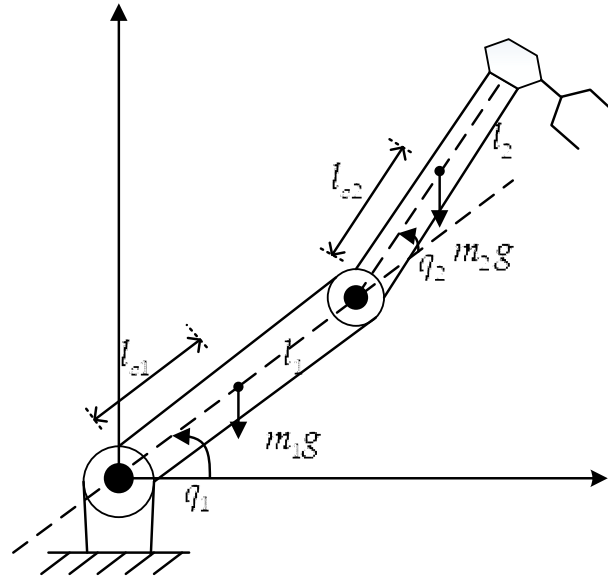


Figure 2. Schematic diagram of a dual-joint robot manipulator. m_i and l_i are the weight and length of the link i , respectively. l_{ci} represents the distance between the center of mass of link $i - 1$ and joint i , $i = 1, 2$.

The position vector is defined as $q = [q_1 \ q_2]^T$. According to reference [22], the correlation matrixes of dynamics equations are given below:

$$M(q) = \begin{bmatrix} M_{11} & M_{12} \\ M_{21} & M_{22} \end{bmatrix} \quad (35)$$

$$C(q, \dot{q}) = \begin{bmatrix} C_{11} & C_{12} \\ C_{21} & C_{22} \end{bmatrix} \quad (36)$$

$$G(q) = [G_{11} \ G_{21}]^T \quad (37)$$

$$J(q) = \begin{bmatrix} -(l_1 \sin q_1 + l_2 \sin(q_1 + q_2)) & -l_2 \sin(q_1 + q_2) \\ l_1 \cos q_1 + l_2 \cos(q_1 + q_2) & l_2 \cos(q_1 + q_2) \end{bmatrix} \quad (38)$$

with

$$M_{11} = m_1 l_{c1}^2 + m_2 (l_1^2 + l_{c2}^2 + 2l_1 l_{c2} \cos q_2) + I_1 + I_2$$

$$M_{12} = m_2 (l_{c2}^2 + l_1 l_{c2} \cos q_2) + I_2$$

$$M_{21} = m_2 (l_{c2}^2 + l_1 l_{c2} \cos q_2) + I_2$$

$$M_{22} = m_2 l_{c2}^2 + I_2$$

$$C_{11} = -m_2 l_1 l_{c2} \dot{q}_2 \sin q_2$$

$$C_{12} = -m_2 l_1 l_{c2} (\dot{q}_1 + \dot{q}_2) \sin q_2$$

$$C_{21} = m_2 l_1 l_{c2} \dot{q}_1 \sin q_2$$

$$C_{22} = 0$$

$$G_{11} = (m_1 l_{c1} + m_2 l_1) g \cos q_1 + m_2 l_{c2} g \cos(q_1 + q_2)$$

$$G_{21} = m_2 l_{c2} g \cos(q_1 + q_2)$$

The parameter selection for the robot is $m_1 = 2.00$ kg, $m_2 = 0.85$ kg, $l_1 = 0.35$ m, $l_2 = 0.31$ m, $I_1 = 0.25m_1l_1^2$ kgm², and $I_2 = 0.25m_2l_2^2$ kgm².

The initial conditions set in the simulation are as follows

$$\begin{cases} q_1(0) = 0.1, q_2(0) = 0.2 \\ \dot{q}_1(0) = \dot{q}_2(0) = 0 \end{cases} \quad (39)$$

The setting of the reference path is the same as [6], $x_{d1} = 0.14 \sin(0.5t)$, $x_{d2} = 0.14 \cos(0.5t)$. Select system disturbance as $f(t) = [\sin(t) + 1; 2 \cos(t) + 0.5]$. The parameters of the controller in the experiment are set as $K_1 = \text{diag}[30, 30]$, $K_2 = \text{diag}[30, 30]$, $K_s = 5$. The neural network parameters are selected as follows: $\Gamma_1 = 0.1I_{256 \times 256}$, $\Gamma_2 = 0.1I_{256 \times 256}$, $\sigma_1 = 0.2$, and $\sigma_2 = 0.2$, the initial weights $\hat{W}_{1,i} = 0$, $\hat{W}_{2,i} = 0$, ($i = 1, 2, \dots, 256$), the number of nodes is $N = 256$, and the width of the NN is $\eta = 10$. The gain matrix of the disturbance observer is selected as $l(x) = [0.01 \ 0; 0 \ 0.1]^{-1} M^{-1}(x_1)$. We set the simulation time to 40 s. The controller design for comparison is $\tau = -z_1 - K_2 z_2 - \text{sgn}(z_2^T) \odot J^T(x_1) \bar{f} + \hat{W}^T S(Z)$ [6].

The results of the simulation are depicted in Figures 3–10. Figures 3 and 4 show the trajectory tracking and errors of the two joints. Both methods can guarantee that the tracking error converges to the small neighborhood of zero in a short period of time. After the system reaches a stable state, the tracking error of joint 1 is $z_{11} \approx -9.0 \times 10^{-6}$, and the tracking error of joint 2 is $z_{12} \approx -1.2 \times 10^{-5}$, which is a relatively small value, reflecting the superiority of the proposed method. We can see that the two control algorithms have a significant difference in their position tracking performance. Compared to the method in [6], the tracking errors of z_{11} and z_{12} triggered by the presented control have a higher accuracy. On the one hand, this is attributed to the integral sliding mode surface with the positional error in the adaptive controller (27), which effectively reduces the system's steady-state error. On the other hand, approximate errors can be accurately estimated and compensated by the designed disturbance observer. The velocity-tracking curve is plotted in Figure 5. The control inputs are given in Figure 6. The blue and green lines denote the control input of joint 1, while the red and blue lines denote the control input of joint 2. We can see that even with model uncertainties and disturbances, the inputs of both control methods are smooth and without chatter. Within (0,0.1) seconds, the compared amplitude is greater than the proposed amplitude, indicating that the compared controller needs to consume more energy during the initial tracking stage. In addition, the preset initial position $q(0)$ is not at the expected position $q_d(0)$, which leads to a large initial input value, but it can ensure that the system quickly achieves the desired control effect. Through the further analysis of Figures 3, 4 and 6, it can be concluded that the developed controller improves its tracking accuracy without increasing its energy consumption, which also reflects the superiority of the presented ANN control scheme. The adaptive weights of \hat{W}_1 and \hat{W}_2 are presented in Figure 7. This indicates that the proposed adaptation weights can converge to a positive constant in a short time and achieve a reasonably stable state faster than [6], which also demonstrates the boundedness of the adaptation weights. Figure 8 shows the approximation errors of the two control strategies. It is evident that the presented method has a smaller error and can converge to near zero within 0.3 s. The true value ω_i and the observed value $\hat{\omega}_i$ are shown in Figures 9 and 10. The designed disturbance observer (24) can accurately estimate the approximation errors $\varepsilon(Z)$ and external disturbances $J^T f(t)$, perform real-time compensation on the control input (27), and achieve the expected tracking effect after 0.5 s. This also verifies that the proposed adaptive neural network control algorithm based on the disturbance observer can achieve a good tracking control response in this paper.

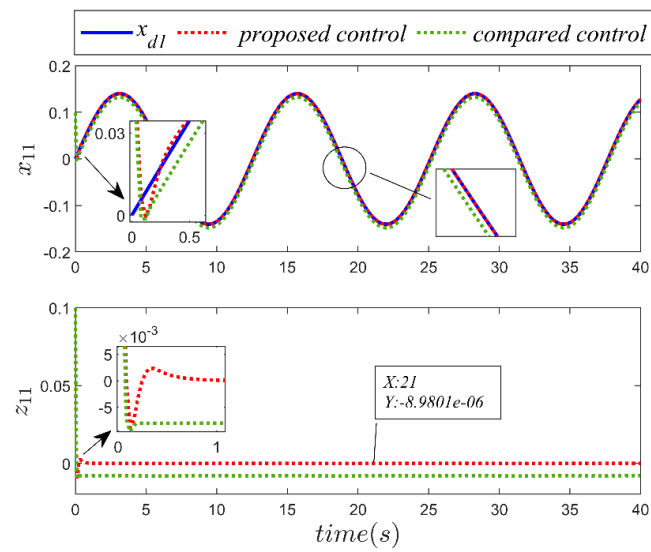


Figure 3. Trajectory tracking of joint 1 and its errors.

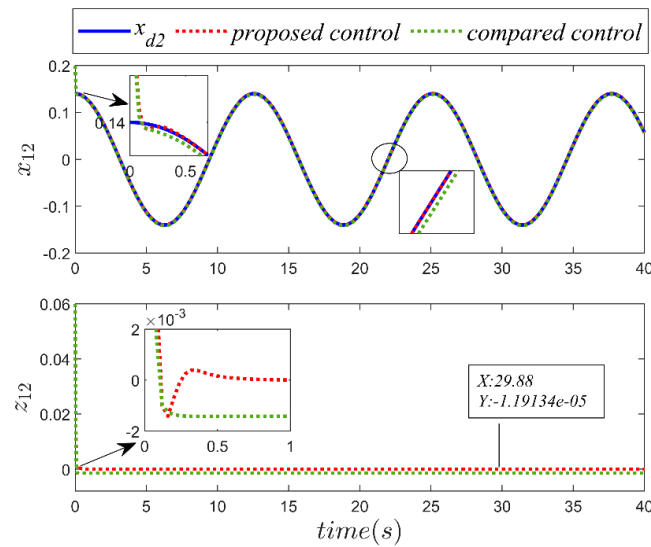


Figure 4. Trajectory tracking of joint 2 and its errors.

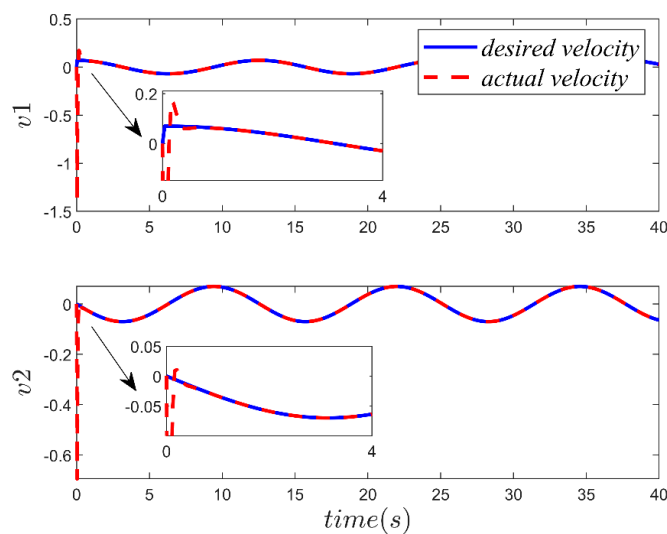


Figure 5. Velocities of joint 1 and joint 2.

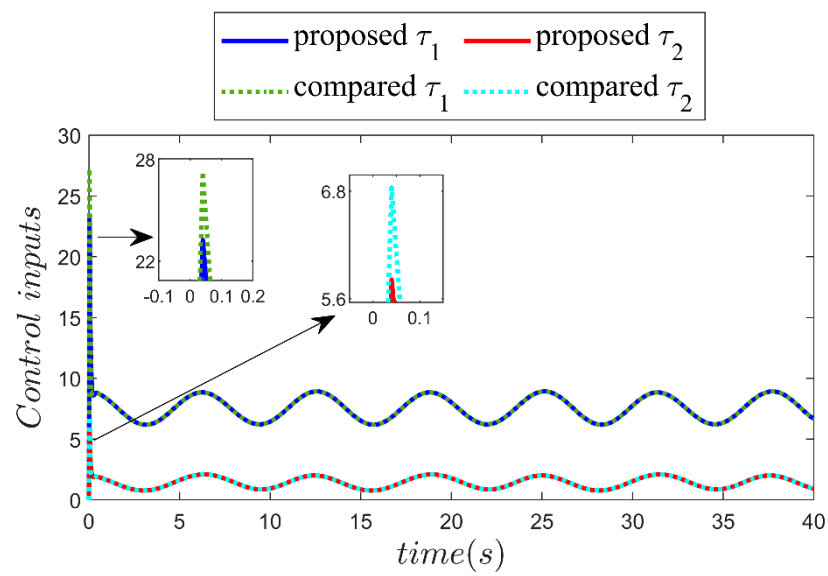


Figure 6. The control inputs for the two methods.

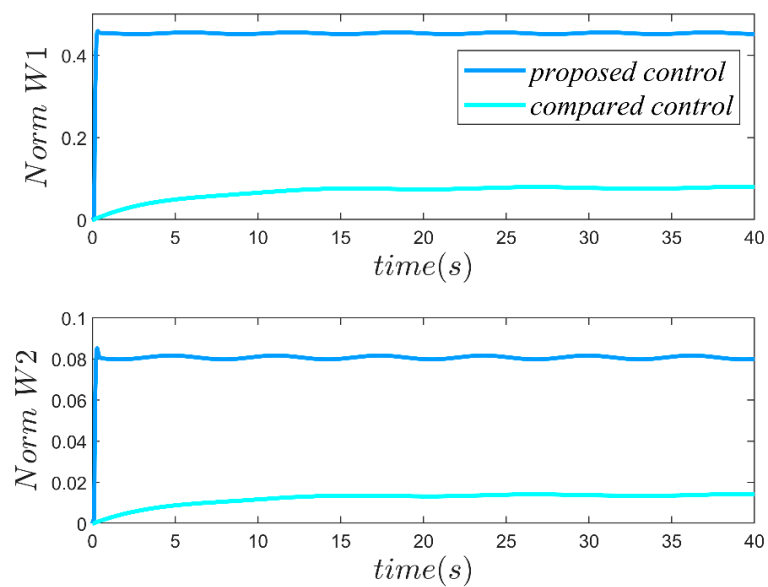


Figure 7. Norms of the adaptation weights under the two methods.

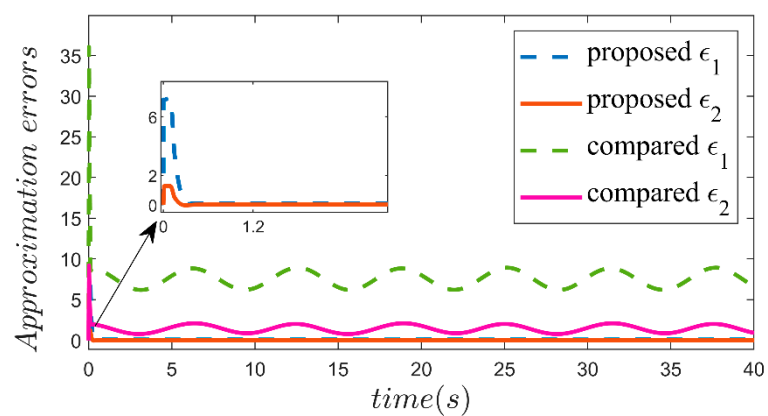


Figure 8. The approximation errors under the two methods.

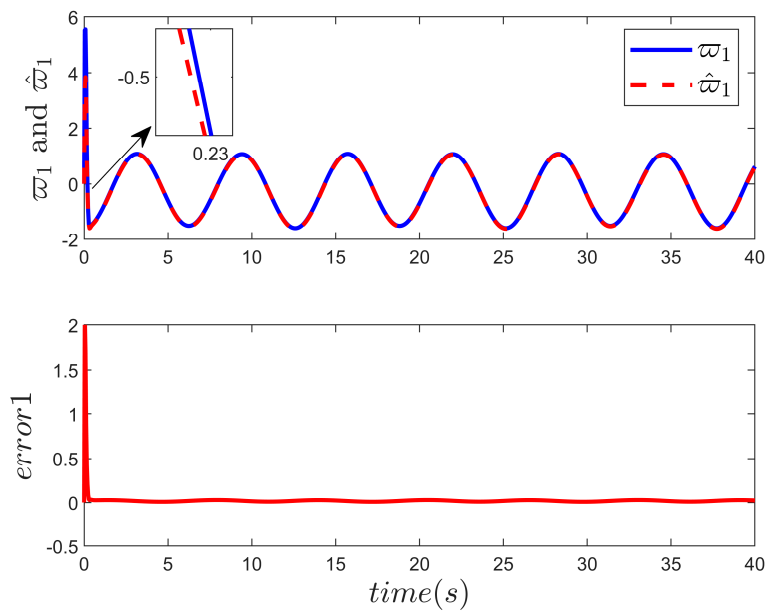


Figure 9. Observation effect of joint 1.

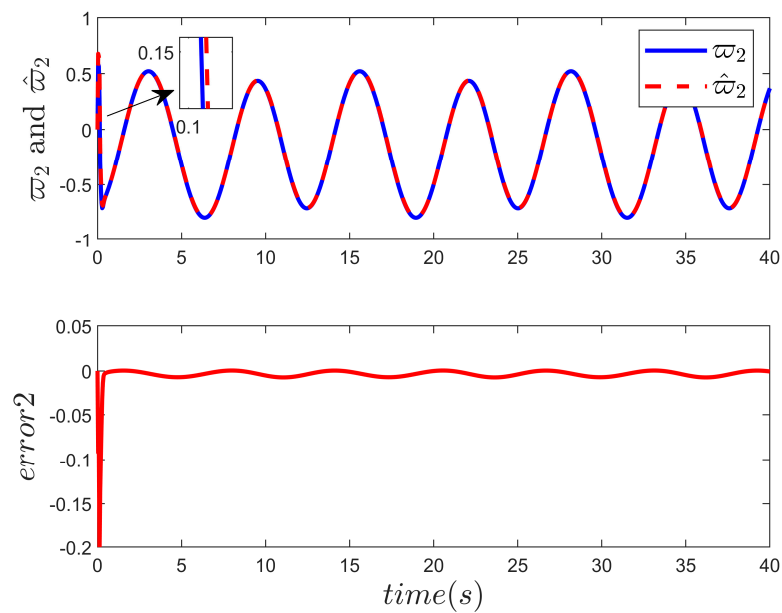


Figure 10. Observation effect of joint 2.

5. Conclusions

An ANN control strategy based on a disturbance observer was developed for the trajectory tracking control of robotic manipulators while considering the dynamic model uncertainties and external disturbances. It has been demonstrated that the proposed control method can ensure the error signal of the closed-loop system is bounded based on the Lyapunov stability theory. An ANN controller based on full-state feedback was designed, which approximates the model uncertainty online and compensates for the controller by adjusting the adaptive update law. When using backstepping technology to derive the controller, an integral sliding mode surface was added to reduce the steady-state error of the system. Then, the state equation of the system was redefined to guarantee the rationality of the observer structure. The bounded values of approximation errors are considered in the observer, which makes the structural design more rational and ensures the overall stability of the system. Furthermore, a disturbance observer was used for the first time to achieve

the accurate estimation of both approximation errors and environmental disturbances, and compensation was provided to the controller to improve tracking performance. Our future work will concentrate on the tracking control of robots with state constraints and unknown time-varying delays.

Author Contributions: Conceptualization, T.L. and G.Z.; methodology, T.L.; software, T.L. and T.Z.; validation, T.L., T.Z. and J.P.; formal analysis, T.L.; investigation, T.L. and J.P.; resources, T.L. and T.Z.; data curation, T.L.; writing—original draft preparation, T.L.; writing—review and editing, T.L.; visualization, T.L. and G.Z.; supervision, G.Z. and T.Z.; project administration, T.L.; funding acquisition, G.Z. All authors have read and agreed to the published version of the manuscript.

Funding: This research was funded by the University Synergy Innovation Program of Anhui Province under Grant No. GXXT-2021-026, and the Smart Agriculture and Forestry and Smart Equipment Scientific Research and Innovation Team (Anhui Undergrowth Crop Intelligent Equipment Engineering Research Center) under Grant No. 2022AH010091.

Data Availability Statement: All data used to support the findings of this study are included within the article.

Conflicts of Interest: The authors declare no conflicts of interest.

References

- Li, C.; Zhao, L.; Xu, Z. Finite-Time Adaptive Event-Triggered Control for Robot Manipulators with Output Constraints. *IEEE Trans. Circuits Syst. II Express Briefs* **2022**, *69*, 3824–3828. [[CrossRef](#)]
- Arteaga-Peréz, M.A.; Pliego-Jiménez, J.; Romero, J.G. Experimental Results on the Robust and Adaptive Control of Robot Manipulators without Velocity Measurements. *IEEE Trans. Control Syst. Technol.* **2020**, *28*, 2770–2773. [[CrossRef](#)]
- Xu, B. Composite neural dynamic surface control of a class of uncertain nonlinear systems in strict-feedback form. *IEEE Trans. Cybern.* **2017**, *44*, 2626–2634. [[CrossRef](#)] [[PubMed](#)]
- Zhang, G.; Pan, J.; Li, T.; Wang, Z.; Wang, D. Fixed-Time Control of a Robotic Arm Based on Disturbance Observer Compensation. *Processes* **2024**, *12*, 93. [[CrossRef](#)]
- Jin, L.; Li, S.; Yu, J.; He, J. Robot manipulator control using neural networks: A survey. *Neurocomputing* **2018**, *285*, 23–34. [[CrossRef](#)]
- He, W.; Ge, S.S.; Li, Y.; Chew, E.; Ng, Y.S. Neural Network Control of a Rehabilitation Robot by State and Output Feedback. *J. Intell. Robot. Syst.* **2015**, *80*, 15–31. [[CrossRef](#)]
- Ivan, L.-S.; Ricardo, P.-A.; Javier, M.-V. Trajectory tracking double two-loop adaptive neural network control for a Quadrotor. *J. Frankl. Inst.* **2023**, *360*, 3770–3799.
- Zhang, Y.; Liu, J.; Yu, J.; Liu, D. Single neural network-based asymptotic adaptive control for an autonomous underwater vehicle with uncertain dynamics. *Ocean Eng.* **2023**, *286*, 115553. [[CrossRef](#)]
- Hassan, N.; Saleem, A. Neural Network-Based Adaptive Controller for Trajectory Tracking of Wheeled Mobile Robots. *IEEE Access* **2022**, *10*, 13582–13597. [[CrossRef](#)]
- Angel, L.; Viola, J. Fractional order PID for tracking control of a parallel robotic manipulator type delta. *ISA Trans.* **2018**, *79*, 172–188. [[CrossRef](#)]
- Zhao, H.; Liu, W.; Chen, X.; Sun, H. Adaptive robust constraint-following control for underactuated unmanned bicycle robot with uncertainties. *ISA Trans.* **2023**, *143*, 144–155. [[CrossRef](#)] [[PubMed](#)]
- Zhen, S.; Meng, C.; Xiao, H.; Liu, X.; Chen, Y.-H. Robust approximate constraint following control for SCARA robots system with uncertainty and experimental validation. *Control Eng. Pract.* **2023**, *138*, 105610. [[CrossRef](#)]
- Yu, X.; Li, B.; He, W.; Feng, Y.; Cheng, L.; Silvestre, C. Adaptive-Constrained Impedance Control for Human–Robot Co-Transportation. *IEEE Trans. Cybern.* **2022**, *52*, 13237–13249. [[CrossRef](#)] [[PubMed](#)]
- Duan, J.J.; Gan, Y.H.; Chen, M.; Dai, X.Z. Symmetrical adaptive variable admittance control for position/force tracking of dual-arm cooperative manipulators with unknown trajectory deviations. *Robot. Comput.-Integr. Manuf.* **2019**, *57*, 357–369.
- Liu, Y.; Wang, Y.; Guan, X.; Hu, T.; Zhang, Z.; Jin, S.; Wang, Y.; Hao, J.; Li, G. Direction and Trajectory Tracking Control for Nonholonomic Spherical Robot by Combining Sliding Mode Controller and Model Prediction Controller. *IEEE Robot. Autom. Lett.* **2022**, *7*, 11617–11624. [[CrossRef](#)]
- Truong, T.N.; Vo, A.T.; Kang, H.-J. A Backstepping Global Fast Terminal Sliding Mode Control for Trajectory Tracking Control of Industrial Robotic Manipulators. *IEEE Access* **2021**, *9*, 31921–31931. [[CrossRef](#)]
- Hu, H.; Wang, X.; Chen, L. Impedance Sliding Mode Control with Adaptive Fuzzy Compensation for Robot-Environment Interacting. *IEEE Access* **2020**, *8*, 19880–19889. [[CrossRef](#)]
- Yin, X.X.; Pan, L.; Cai, S.B. Robust adaptive fuzzy sliding mode trajectory tracking control for serial robotic manipulators. *Robot. Comput.-Integr. Manuf.* **2021**, *72*, 101884. [[CrossRef](#)]
- Zaare, S.; Soltanpour, M.R. Adaptive fuzzy global coupled nonsingular fast terminal sliding mode control of n-rigid-link elastic-joint robot manipulators in presence of uncertainties. *Mech. Syst. Signal Process.* **2022**, *163*, 108165. [[CrossRef](#)]

20. Truong, T.N.; Vo, A.T.; Kang, H.-J. Neural network-based sliding mode controllers applied to robot manipulators: A review. *Neurocomputing* **2023**, *562*, 126896. [[CrossRef](#)]
21. Yang, C.; Huang, D.; He, W.; Cheng, L. Neural Control of Robot Manipulators with Trajectory Tracking Constraints and Input Saturation. *IEEE Trans. Neural Netw. Learn. Syst.* **2022**, *32*, 4231–4242. [[CrossRef](#)] [[PubMed](#)]
22. Sun, W.; Wu, Y.; Lv, X. Adaptive Neural Network Control for Full-State Constrained Robotic Manipulator with Actuator Saturation and Time-Varying Delays. *IEEE Trans. Neural Netw. Learn. Syst.* **2022**, *33*, 3331–3342. [[CrossRef](#)] [[PubMed](#)]
23. Liu, E.; Yan, Y.; Yang, Y. Neural network approximation-based backstepping sliding mode control for spacecraft with input saturation and dynamics uncertainty. *Acta Astronaut.* **2022**, *191*, 1–10. [[CrossRef](#)]
24. Zhang, Y.; Kong, L.; Zhang, S.; Yu, X.; Liu, Y. Improved Sliding Mode Control for a Robotic Manipulator with Input Deadzone and Deferred Constraint. *IEEE Trans. Syst. Man Cybern. Syst.* **2023**, *53*, 7814–7826. [[CrossRef](#)]
25. Singh, P.; Giri, D.K.; Ghosh, A.K. Robust backstepping sliding mode aircraft attitude and altitude control based on adaptive neural network using symmetric BLF. *Aerosp. Sci. Technol.* **2022**, *126*, 107653. [[CrossRef](#)]
26. Vijay, M.; Jena, D. Backstepping terminal sliding mode control of robot manipulator using radial basis functional neural networks. *Comput. Electr. Eng.* **2018**, *67*, 690–707. [[CrossRef](#)]
27. Gao, X.; Yu, H.; Yang, Q.; Meng, X.; Zhang, P. Neural network based dynamic surface integral nonsingular fast terminal sliding mode control for manipulators with disturbance rejection. *J. Frankl. Inst.* **2023**, *360*, 11032–11054. [[CrossRef](#)]
28. Ding, Z.; Wang, H.; Sun, Y.; Qin, H. Adaptive prescribed performance second-order sliding mode tracking control of autonomous underwater vehicle using neural network-based disturbance observer. *Ocean Eng.* **2022**, *260*, 111939. [[CrossRef](#)]
29. Men, X.; Guo, Z. Adaptive composite control of an upper limb compliant exoskeleton robot based on RBF neural network. *Control Eng. China* **2023**, *6*, 1–9.
30. Zhang, R.; Xu, B.; Shi, P. Output Feedback Control of Micromechanical Gyroscopes Using Neural Networks and Disturbance Observer. *IEEE Trans. Neural Netw. Learn. Syst.* **2022**, *33*, 962–972. [[CrossRef](#)]
31. Li, G.; Yu, J.; Chen, X. Adaptive Fuzzy Neural Network Command Filtered Impedance Control of Constrained Robotic Manipulators with Disturbance Observer. *IEEE Trans. Neural Netw. Learn. Syst.* **2023**, *34*, 5171–5180. [[CrossRef](#)]
32. He, W.; Dong, Y.; Sun, C. Adaptive neural impedance control of a robotic manipulator with input saturation. *IEEE Trans. Syst. Man Cybern. Syst.* **2016**, *46*, 334–344. [[CrossRef](#)]
33. Li, Y.N.; Yang, C.G.; Ge, S.S.; Lee, T.H. Adaptive output feedback NN control of a class of discrete-time MIMO nonlinear systems with unknown control directions. *IEEE Trans. Syst. Man Cybern. Part B* **2011**, *41*, 507–517.

Disclaimer/Publisher’s Note: The statements, opinions and data contained in all publications are solely those of the individual author(s) and contributor(s) and not of MDPI and/or the editor(s). MDPI and/or the editor(s) disclaim responsibility for any injury to people or property resulting from any ideas, methods, instructions or products referred to in the content.